Journal of Solid State Chemistry **166,** 362–368 (2002)
doi:10.1006/jssc.2002.9606

Synthesis and Structure of the New Ammonium Indium Phosphate $(NH_4)In(OH)PO_4$

A. A. Filaretov,* M. G. Zhizhin,† L. N. Komissarova,† V. P. Danilov,* V. V. Chernyshev,† and B. I. Lazoryak†,[1]

*Institute of General and Inorganic Chemistry, Russian Academy of Sciences, 117907 Moscow, Russia; and †Department of Chemistry, Moscow State University, 119899 Moscow, Russia

Received December 1, 2001; in revised form March 25, 2002; accepted April 5, 2002

A new ammonium indium phosphate $(NH_4)In(OH)PO_4$ was prepared by hydrothermal reaction in the In_2O_3–$NH_4H_2PO_4$–NH_3/OH system ($T = 200°C$, autogenous pressure, 7 days). The formula $(NH_4)In(OH)PO_4$ was determined on the basis of chemical and thermal analysis (TG/DSC), X-ray powder diffraction and IR-spectroscopy. $(NH_4)In(OH)PO_4$ crystallizes in the tetragonal system with space group $P4_32_12$ (No. 96); $a = 9.4232(1)$ Å, $c = 11.1766(1)$ Å, $V = 992.45(2)$ Å^3; $Z = 8$. The crystal structure was refined by the Rietveld method ($R_w = 6.35\%$, $R_p = 5.10\%$). The second-harmonic generation study confirmed that structure of $(NH_4)In(OH)PO_4$ does not have a center of symmetry. The *cis*-$InO_4(OH)_2$ octahedra form helical chains, parallel to the *c*-axis. The In–O–In bonds are nearly equidistant. The chains are interconnected by phosphate tetrahedra and create tunnels containing the NH_4^+ ions along the *c*-axis. $(NH_4)In(OH)PO_4$ is isostructural with $RbIn(OH)PO_4$. © 2002 Elsevier Science (USA)

Key Words: **indium phosphate; crystal structure; Rietveld method; IR spectroscopy; second harmonic generation.**

INTRODUCTION

At present, the increasing interest in the synthesis and structural characterization of new complex phosphates is due largely to diversity of structure types and abundance of metal phosphate framework compounds as well as to their potential applications as new materials that may have interesting physical, electronic and magnetic properties (1, 2). In contrast to the very well-known aluminophosphates and gallophosphates with metallic atoms in four-, five- or six-fold coordination, there is very scant information on complex indium phosphates in the literature, namely, α- and β-$Li_3In_2(PO_4)_3$ (3,4), $LiInP_2O_7$ (5), $NaCdIn_2(PO_4)_3$ (6), $CsIn_2(PO_4)(HPO_4)_2(H_2O)_2$ (7), AIn(OH)PO_4 (A = K, Rb) (8, 9), α- and β-$Na_3In(PO_4)_2$ (10, 11), α- and β-$Na_3In_2(PO_4)_3$ (12, 13), $CaIn_2(PO_4)_2(HPO_4)$ (14), $Ba_3In_2(HPO_4)_6$ (15), $Na_4In_8(HPO_4)_{14}(H_2O)_6 \cdot 12H_2O$ (16) and $Na_2In_2(HPO_4)_4 \cdot H_2O$ (17). In these compounds the indium has only octahedral coordination. Most of the described compounds have been synthesized by either hydrothermal or solid-state reactions. The crystal structures of AIn(OH)PO_4 (A = K, Rb) were studied by using the single crystals which were obtained by the high-pressure hydrothermal method ($T = 900°C$ and 550°C, respectively). KIn(OH)PO_4 with a structural formula similar to that of the important nonlinear optical (NLO) material $KTiOPO_4$ (KTP) (18) has a different structure and does not demonstrate an NLO effect.

This paper describes a low-temperature hydrothermal synthesis, structural characterization and spectroscopic/optical properties of the new phosphate $(NH_4)In(OH)PO_4$.

EXPERIMENTAL

Preparation

The $(NH_4)In(OH)PO_4$ compound was prepared by the mild hydrothermal method. The reactants were indium oxide (In_2O_3), ammonium phosphate ($NH_4H_2PO_4$) and ammonium hydroxide (NH_3/H_2O) of analytical grade. The mixture of In_2O_3, $NH_4H_2PO_4$, NH_3/H_2O (starting mole ratio of NH_4^+:In^{3+}: $PO_4^{3-} = 8.10:1:2.41$) and H_2O was placed in a Teflon-lined stainless-steel autoclave and was heated at 200°C for 24 h under autogenous pressure with volume filled by 75%. The pH, initially ca. 10, lowered to 7.5 at the end of the reaction. An experiment was carried out with a longer reaction time (7 days). The autoclave was slowly cooled at 10°C h^{-1} down to 40°C and quenched to room temperature by removing the autoclave from the furnace. The powdered product was filtered, washed with distilled water and acetone, and finally dried in air at

[1]To whom correspondence should be addressed. Fax: +7-095-938-2457. E-mail: lazoryak@tech.chem.msu.ru.

0022-4596/02 $35.00

ambient temperature. X-ray powder diffraction pattern of the white polycrystalline product showed that it was a single phase and highly crystalline.

Characterization

The as-synthesized product was characterized by X-ray powder diffraction (XRD) at room temperature using a STOE STADI-P powder diffractometer equipped with a primary germanium (111) monochromator ($CuK\alpha_1$ radiation, $\lambda = 1.5406$ Å), and a position sensitive detector. The data were collected over the range of 5–100° (2θ) with a step of 0.01°, and the effective counting time was ca. 30 min per step.

A thermal investigation was performed by combining information from thermogravimetric (TG) and differential scanning calorimetric (DSC) measurements between 20°C and 850°C using a heating and cooling rate of 10°C min^{-1}. The TG was performed using a derivatograph OD-103. The DSC data were collected from powder sealed in aluminum pans using a Rheometric Sciences DSC 1000 calorimeter.

Infrared spectrum was collected on a Nicolet Magna-750 Fourier spectrometer in the range of 400–4000 cm^{-1}. The analysis of spectra was carried out in the area of PO_4^{3-} and OH^- groups oscillations.

The second-harmonic generation (SHG) response of powder sample was measured using the reflection mode. A Q-switch pulsed Nd:YAG laser operating at $\lambda_\omega = 1064$ nm was used as the radiation source with a repetition rate of 4 pulses s^{-1} and a pulse duration of about 12 ns. The laser beam was split into two beams to excite the radiation at a doubled frequency ($\lambda_{2\omega} = 532$ nm) simultaneously in the phosphate sample and reference, α-SiO_2. The maximum power of the incident beam was about 0.1 MW on a spot 3 mm in diameter on the surface of the sample.

RESULTS AND DISCUSSION

Chemical Analysis

The chemical analysis of indium and phosphorus was performed on 100 and 300 mg of material, respectively. Reverse titration of (EDTA) ethylenediaminetetraacetic acid excess by $CuSO_4$ solution with PÀN indicator in the acetate buffer was used to determine the indium concentration. The phosphorus content was measured by spectrophotometry. The sample was evacuated in a desiccator at room temperature overnight in order to withdraw adsorbed H_2O. The chemical analysis gave: In, 46.19; P, 11.69 (wt%). These results are in fair agreement with the theoretical values calculated for the chemical formula $(NH_4)In(OH)PO_4$ (In: 46.90, P: 12.65%). The In/P molar ratio, equal to 1.07, is close to that derived from the formula (In/P = 1).

The experimental density found by pycnometer in carbon tetrachloride for $(NH_4)In(OH)PO_4$ is 3.26(1) g cm^{-3}. This result is in good agreement with the theoretical value 3.28 g cm^{-3} calculated for eight $(NH_4)In(OH)PO_4$ formula units per unit cell from X-ray powder data.

Thermal Analysis

Two distinct weight losses could be seen on the TG curves of the as-synthesized $(NH_4)In(OH)PO_4$ sample. The first one, recorded between 180°C and 490°C (~10.31 wt%), is attributed to the elimination of NH_3 gas and 0.5 mol of H_2O. The removal of the NH_3 species is accompanied by one endothermic peak around 300°C, but this event is just discernible. The second weight loss (~4.36 wt%), occurring between 535°C and 630°C, is presumably due to water loss resulting from the decomposition of hydroxide (In–OH–In) group together with the remaining hydrogen after a breakdown of the ammonium cation. An endothermic peak around 560°C accompanied the removal of water. The endothermic peak was followed by an exothermic peak (620°C), reflecting the formation of $InPO_4$. The weight loss is relatively close to the one expected (14.33 wt%) according to Eq. (1) and there is no bound water in $(NH_4)In(OH)PO_4$. At higher temperature, the compound converts from an amorphous into a crystalline phase and the X-ray powder result for the final sample at 800°C shows good crystallization of the indium phosphate (JCSPD, PDF # 72-1132).

$$(NH_4)In(OH)PO_4 \rightarrow InPO_4 + NH_3 + H_2O. \qquad [1]$$

Infrared Spectroscopy

Figure 1 shows the IR spectrum of $(NH_4)In(OH)PO_4$. The observed frequencies correspond to the characteristic frequencies of the PO_4, NH_4 and OH groups. In the OH valence vibration region of 3700–3500 cm^{-1}, the spectrum displays one major sharp absorption band around 3537 cm^{-1} due to stretching of the OH group attached to indium. The position of the OH valence stretching vibration is the same as that of $RbIn(OH)PO_4$ compound—3520 cm^{-1} (9). The bands assigned to the characteristic stretching and deformation vibrations of water molecules are not observed in the IR spectrum of $(NH_4)In(OH)PO_4$.

Bands arising from NH_4^+ cations are also seen. The broad and weak bands between 3230 and 3020 cm^{-1} are assigned to the stretching vibrations of ammonium cation. The further free absorption bands in the 3000–2850 cm^{-1} region are very difficult to define, despite the fact that we

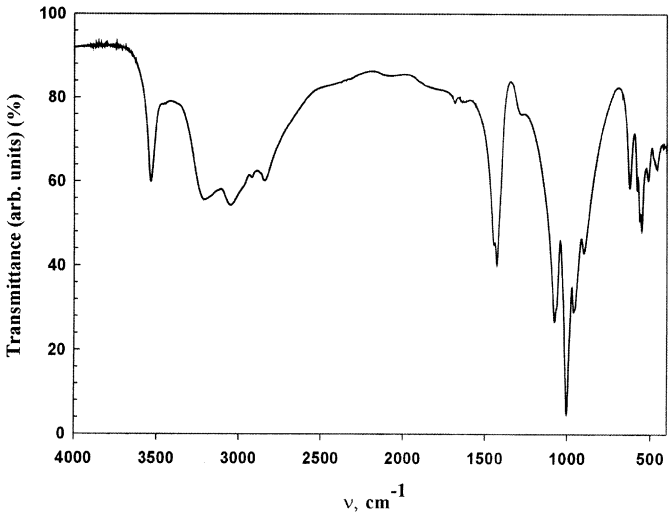

FIG. 1. Infrared spectra of $(NH_4)In(OH)PO_4$.

know in detail the structure of the examined material. In the NH_4-bending region, the two major bands centered around 1447 and 1427 cm^{-1} can be easily related to the triple-degenerated asymmetric bending mode (v_4) (19, 20).

The free PO_4^{3-} tetrahedron exhibits T_d symmetry and therefore possesses four normal modes of vibration having A_1 (v_1 mode), E (v_2) and F_2 (v_3 and v_4) symmetries with average wave numbers of 938, 420, 1017 and 567 cm^{-1}, respectively (20). The v_1 and v_2 modes represent the symmetric stretching and deformation vibrations, while v_3 and v_4 represent the corresponding asymmetric stretching and deformation vibrations. Indeed, the positions of the bands in the spectral region 1100–930 cm^{-1} are typical of the asymmetrical and symmetrical stretching vibrations of PO_4^{3-} group (Table 1) (21–23). The band that was observed at 962 cm^{-1} confirms the presence of only one crystallographic PO_4 group in the compound. The In–O–H bending modes of vibration may explain the bands at 900 cm^{-1}. The following bands, from 650 to 420 cm^{-1}, are probably related mainly to the v_2 and v_4 modes of the PO_4 group, with the exception of the 512 and 458 cm^{-1} bands that possibly correspond to the vibration modes involving In^{3+}.

TABLE 1
Observed IR Vibrational Frequencies (cm^{-1}) for $(NH_4)In(OH)PO_4$

Assignment	PO_4^{3-}	Assignment	NH_4^+
v_{2E}	—	v_{4F2}	1427 s; 1447 sh
v_{4F2}	551 m; 564 sh; 579 sh; 623 m	v_{2E}	1684 sh
v_{1A}	962 s	v_{1A}	3066 mb
v_{3F2}	1003 vs; 1066 sh; 1076 s	v_{3F2}	3227 mb

Note. Relative intensities: vs, very strong; s, strong; m, medium; mb, medium broad; sh, short.

Structure Determination

The tetragonal cell dimension of $(NH_4)In(OH)PO_4$ sample was unambiguously determined with TREOR90 (24) using the first 35 peak positions from the X-ray pattern. Least-squares minimization led to refined lattice parameters of $a = 9.4209(2)$ Å, $c = 11.1739(5)$ Å (figures of merit: $M_{30} = 70$, $F_{30} = 158$ (0.0045, 42)). Index results for $(NH_4)In(OH)PO_4$ will be published in the Powder Diffraction File. Two possible space groups $P4_32_12$ (no. 96) and $P4_12_12$ (no. 92) were determined on the basis of systematic absence indexes ($0\,0\,l : l = 4n, h\,0\,0 : h = 2n$).

A comparison of reflex positions of $(NH_4)In(OH)PO_4$ compound with the theoretical X-ray pattern calculated for $RbIn(OH)PO_4$ (9) proves the close similarities and points out the isostructural character of these compounds. The phosphate $RbIn(OH)PO_4$ crystallizes in the tetragonal space group $P4_32_12$ and $Z = 8$. The powder sample $(NH_4)In(OH)PO_4$ showed an SHG response, $I_{2\omega}/I_{2\omega}(SiO_2) \sim 2.8$. This nonzero response is strongly indicative of a noncentrosymmetric space group and is consistent with the successful refinement described below. The structure of $(NH_4)In(OH)PO_4$ was refined in the noncentric space group $P4_32_12$ by using the atomic positions of the $RbIn(OH)PO_4$ compound as a starting model with nitrogen replacing the rubidium.

All calculations were carried out with the updated MRIA program (25). The split-type Psevdo-Voigt peak profile function (26) was used for X-ray powder data. The background was approximated by a Chebyshev polynomial. March-Dollase (27) and symmetrized harmonics expansion (28, 29) texture formalisms were used while processing the X-ray pattern.

The direct methods gave the location of the indium atoms. The position and orientation of PO_4^{3-} anion were found with the grid search procedure (30). Five atoms with the overall temperature factor $B_{iso} = 4$ Å^2 as well as 50 X_{obs} values were used in a search of the first approximation for the best PO_4^{3-} tetrahedra position. The grid increments were taken as 2 Å for molecule translations along a, b, c and 10° for the three rotations. The total number of checked molecule positions was 6859. The PO_4^{3-} group position with $R(X) = 25\%$ was used as initial model in the subsequent Rietveld refinement (RR).

The position and orientation of the NH_4^+ cation was tested applying the grid search procedure by using the hydrogen atomic positions around nitrogen atoms of the KTP-isotype NH_4FeFPO_4 (31) as initial coordinates. The 100 X_{obs} values were involved in a search, and appropriate ammonium position with $R(X) = 10.6\%$ was used in subsequent bond-restrained RR as initial model. During

TABLE 2
Crystallographic Data, Recording Conditions, and Refinement Results for $(NH_4)In(OH)PO_4$

Empirical formula	$In_1P_1O_5N_1H_5$
M	244.84
Temperature (K)	296
Wavelength	Cu$K\alpha_1$ (1.54056 Å)
Crystal system	Tetragonal
Space group	$P4_32_12$ (no. 96)
Unit cell dimensions	
a (Å)	9.4232(1)
c (Å)	11.1766(1)
V (Å^3)	992.45(2)
Z	8
Density (calc./exp.)	3.28/3.26(1) g cm^{-3}
2Θ range (°)	5–100
Step scan increment	0.01
I_{max}	31217
Profile shape function	Psevdo-Voigt
Number of reflections	335
Number of parameters	78
Reliability factors (%)	
R_w[a]	6.35
R_p[b]	5.10
R_b[c]	7.88

[a] $R_w = 100 \times \sum_w [y_{(obs.)} - y_{(cal.)}]^2 / \sum_w [y_{(obs.)}]^{21/2}$.
[b] $R_p = 100 \times \sum |y_{(obs.)} - y_{(cal.)}| / \sum y_{(obs.)}$.
[c] $R_b = 100 \times \sum |y_{(obs.)} - y_{(cal.)}| / \sum |y_{(obs.)} - \text{background}|$.

the bond-restrained RR the H-atoms in ammonium tetrahedra were rigidly connected with the nitrogen atoms. The overall temperature factor of non-H atoms was refined while $U_{iso} = 4$ Å^2 was fixed for all H atoms.

The results of the RR with different texture corrections (March-Dollase and symmetrized harmonics expansion) revealed no texture in powder sample. The occupancy factor for indium positions was allowed to refine but did not deviate significantly from full occupation. It was not possible to locate the hydrogen atoms from difference Fourier data in this structure. The results of full-pattern-decomposition (FPD) and (RR) procedures are $\chi^2 = 3.24$, $R_b = 7.57\%$, $R_p = 4.95\%$ and $\chi^2 = 2.60$, $R_b = 7.88\%$, $R_p = 5.10\%$, $R_w = 6.35\%$, respectively. Details for the final refinements are given in Table 2. Figure 2 shows the Rietveld plot with a good agreement between the observed and the calculated patterns.

Structure Description

The resulting atomic coordinates including isotropic temperature parameters, and a selection of bond distances and angles are shown in Tables 3 and 4, respectively. Both indium atoms sit on two-fold rotation axes and all other atoms are at general positions. Bond-length, bond-strength calculations (32) precisely indicate that the oxygen O5 atom is considerably undersaturated. It is probable that O5 is a hydroxide rather than an oxide ion because its valence sum is equal to 1, and therefore a hydrogen atom must be included to charge balance (see Table 5). Bond valence sum (BVS) values for both the indium and phosphorus atoms show a good chemical connection with respect to the principle of local charge balance. The redundant negative charge of the oxygen atoms O1–O4 proves their participation in the formation of hydrogen bonds with nitrogen atoms.

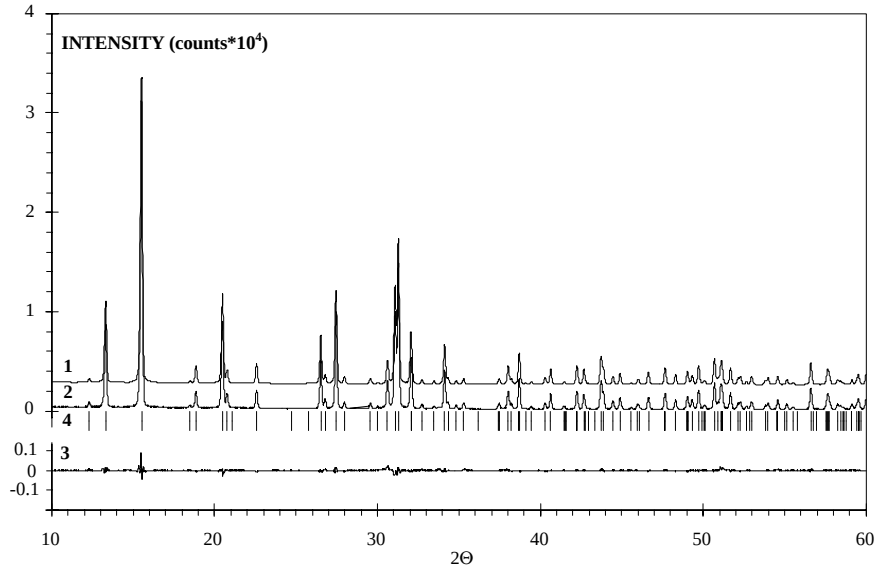

FIG. 2. Portion of the Rietveld refinement profiles for $(NH_4)In(OH)PO_4$: 1—calculated, 2—observed, 3—difference X-ray powder diffraction patterns and 4—Bragg reflections. The calculated pattern is shifted to 2500 counts from the observed pattern.

TABLE 3
Atomic Positions and Thermal Parameters for $(NH_4)In(OH)PO_4$

Atoms	Wyckoff positions	x	y	z	B_{iso}
In1	4*a*	0.09871(4)	0.09871(4)	0	2.41(1)
In2	4*a*	0.65326(4)	0.65326(4)	0	2.37(1)
P	8*b*	0.3356(1)	0.8094(1)	0.9953(2)	3.22(3)
O1	8*b*	0.2799(3)	0.7477(3)	1.1110(2)	3.49(4)
O2	8*b*	0.2721(3)	0.9563(2)	0.9682(2)	3.49(4)
O3	8*b*	0.4980(2)	0.8217(3)	0.9976(3)	3.49(4)
O4	8*b*	0.2944(3)	0.7127(3)	0.8882(2)	3.49(4)
O5	8*b*	0.9479(3)	0.0105(3)	0.8750(2)	2.85(7)
N	8*b*	0.4901(3)	0.1690(3)	0.9557(3)	3.49(4)
H1[a]	8*b*	0.450	0.248	0.943	4
H2[a]	8*b*	0.478	0.115	0.896	4
H3[a]	8*b*	0.454	0.129	1.016	4
H4[a]	8*b*	0.578	0.181	0.967	4

[a] The coordinates and equivalent isotropic factors were fixed.

TABLE 5
Bond Valence Analysis of $(NH_4)In(OH)PO_4$

	In1	In2	P	$\sum s$	Charge
O1	—	0.49×2	1.28	**2.26**	2
O2	0.52×2	—	1.20	**2.24**	2
O3	—	0.50×2	1.21	**2.21**	2
O4	0.53×2	—	1.15	**2.21**	2
O5	0.50	0.50	—	**1.00**	2
O5′	0.50	0.50	—	**1.00**	2
$\sum s$	**3.11**	**2.97**	**4.84**		
Charge	3	3	5		

Note. The results refer to the equation $s = \exp[(R_o - d)/0.37]$ (32) with $R_o = 1.902$ and 1.604 for In^{III}–O and P^{V}–O, respectively.

The $(NH_4)In(OH)PO_4$ compound crystallizes in the noncentrosymmetric space group $P4_32_12$. The structure of $(NH_4)In(OH)PO_4$ is built up from the connection of helical chains of *cis* coner-shared $InO_4(OH)_2$ octahedra which run along the *c*-axis (Fig. 3). The In1 and In2 atoms are arranged in alternate order along the helical chain. There are four $InO_4(OH)_2$ octahedra per helix along the length of the *c*-axis. The phosphate groups link together the indium–oxide–hydroxide chains but do not form contacts between the tetrahedral phosphate groups. The asymmetric unit consists of two PO_4 tetrahedra sharing two of their corners with two $InO_4(OH)_2$ octahedra and the remaining two

TABLE 4
Interatomic Distances (Å) and Angles (deg) in $(NH_4)In(OH)PO_4$

In1	O2	O2′	O4	O4′	O5	O5′
$In1O_6$ octahedron						
O2	**2.144(2)**	*	2.968(2)	3.073(4)	3.268(4)	3.026(4)
O2′	168.9(1)	**2.144(2)**	3.073(4)	2.968(2)	3.026(4)	3.268(4)
O4	80.5(1)	91.8(1)	**2.134(3)**	3.091(5)	3.090(3)	*
O4′	91.8(1)	80.5(1)	92.8(1)	**2.134(3)**	*	3.090(3)
O5	98.8(1)	89.3(1)	92.1(1)	168.9(2)	**2.159(3)**	2.916(2)
O5′	89.3(1)	98.8(1)	168.9(2)	92.1(1)	84.9(1)	**2.159(3)**
			⟨In1–O⟩ = 2.146			
In2	O1	O1′	O3	O3′	O5	O5′
$In2O_6$ octahedron						
O1	**2.169(3)**	3.129(5)	3.158(6)	2.869(3)	3.166(3)	*
O1′	92.3(1)	**2.169(3)**	2.869(3)	3.158(6)	*	3.166(3)
O3	93.7(1)	83.0(2)	**2.159(1)**	*	2.914(7)	3.277(2)
O3′	83.0(2)	93.7(1)	175.4(1)	**2.159(1)**	3.277(2)	2.914(7)
O5	93.9(2)	166.7(1)	84.9(1)	98.6(2)	**2.162(3)**	2.849(5)
O5′	166.7(1)	93.9(2)	98.6(2)	84.9(1)	82.4(1)	**2.162(3)**
			⟨In2–O⟩ = 2.163			
					In1–O5–In2 118.0(3)	
P	O1	O2	O3	O4		
PO_4 tetrahedron						
O1	**1.512(3)**	2.533(3)	2.514(4)	2.516(5)		
O2	112.3(1)	**1.538(1)**	2.500(3)	2.472(2)		
O3	111.2(1)	108.9(1)	**1.535(2)**	2.496(4)		
O4	110.3(1)	106.2(1)	107.8(1)	**1.554(3)**		
			⟨P–O⟩ = 1.535			

Note. * The distances between the *trans*-oxygen atoms are not shown.

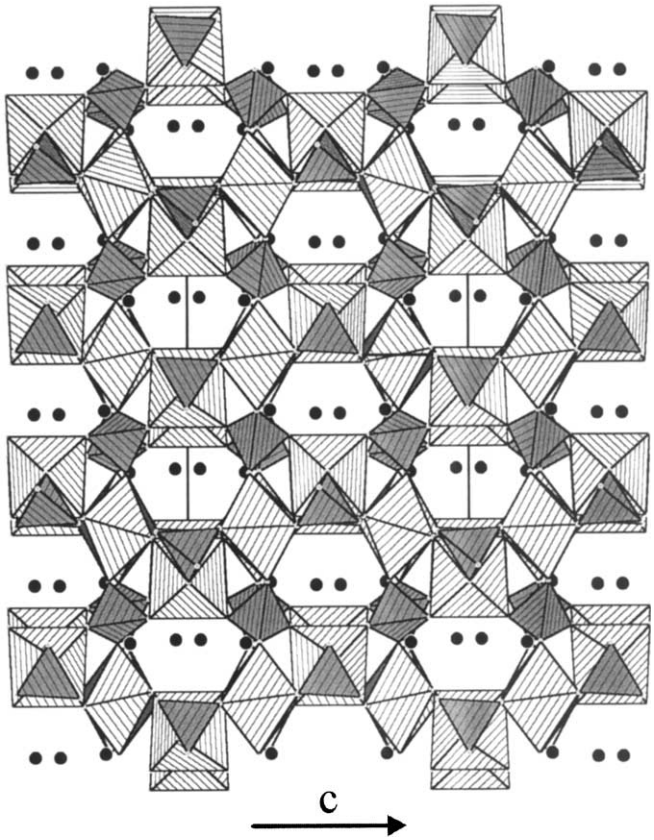

FIG. 3. A layer in the structure of $(NH_4)In(OH)PO_4$ projected down [110], showing chains of $InO_4(OH)_2$ octahedra linked by PO_4 tetrahedra.

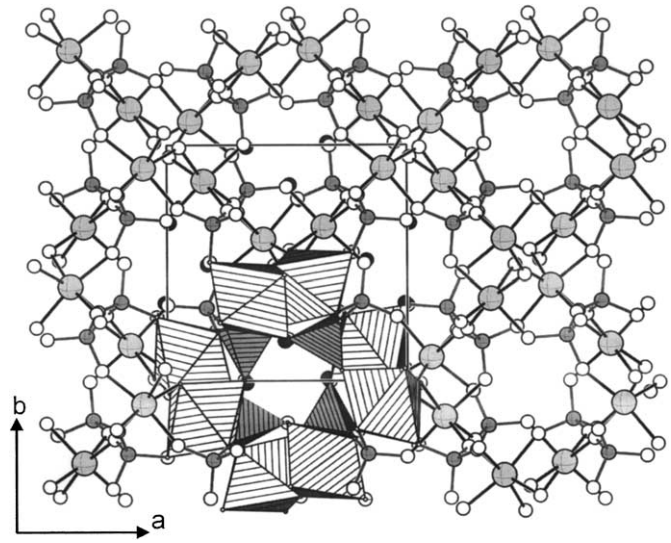

FIG. 5. Projection [001] of the structure $(NH_4)In(OH)PO_4$ showing the square channels (the black circles are nitrogen atoms in the unit cell) parallel to the *c*-axis.

oxygen vertices of PO_4 tetrahedra are connected with two adjacent octahedra in neighboring helices. (Fig. 4). Together, $InO_4(OH)_2$ octahedra and PO_4 tetrahedra form a three-dimensional network with infinite channels along the [110] and [001] directions, where NH_4^+ cations are entrapped in cavities of the indium phosphate skeleton to balance the framework negative charge. The presence of NH_4^+ cations has been earlier proved by IR spectroscopy. The cavities are interconnected so that channels are formed parallel to the *c*-axis with practically square windows and a diagonal that varies between 3.51 and 3.33 Å (Fig. 5). Four helices connected with each other by means of screw axes 4_3, surrounding each of the channels.

The two distinct indium sites in $(NH_4)In(OH)PO_4$ are both octahedral and the $In1O_4(OH)_2$ and $In2O_4(OH)_2$ groups are quite regular. The distortion of indium octahedra may be estimated by the parameter $\Delta = \sum_i \times ((R_i - R_m)/R_m)2/6$, where R_i corresponds to an individual bond length and R_m to an average one (33). The calculation gives $\Delta In1 = 2.29 \times 10^{-5}$ and $\Delta In2 = 3.776 \times 10^{-6}$, which is comparable with the value found for $RbIn(OH)PO_4$ ($\Delta In1 = 7.49 \cdot 10^{-5}$ and $\Delta In2 = 6.65 \times 10^{-6}$), accordingly.

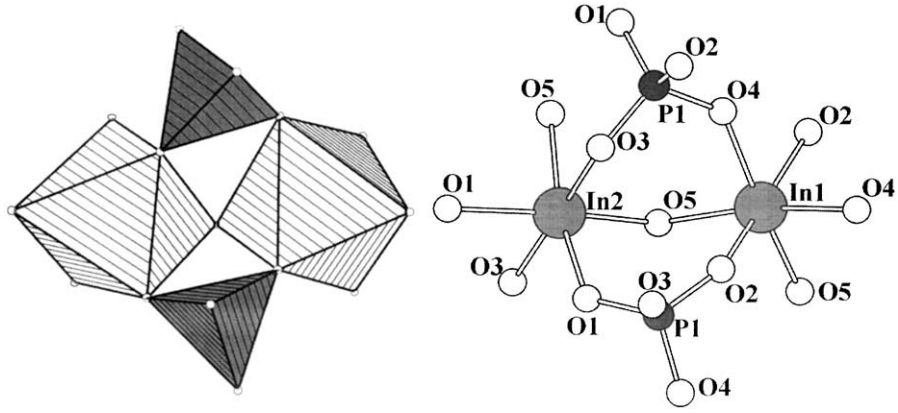

FIG. 4. Indium coordination environment in $(NH_4)In(OH)PO_4$.

The average indium to oxygen bond distances [d_{av}(In1−O) = 2.146 Å, d_{av}(In2−O) = 2.163 Å] accord well with the bond distances expected for these species on the basis of ionic-radii sums (33). BVS values for In1 (3.11) and In2 (2.97) are close to those observed for trivalent indium. These two distinct indium atoms are linked together via a hydroxide oxygen atom O5 and there is no observed short In–O linkage as is the case for the Ti = O titanyl bond of $KTiOPO_4$ (34). The phosphorus atom is in tetrahedral coordination with average P–O distance of 1.535 Å (BVS = 4.84) and average bond angle of 109.5° is commensurate with the ideal value of 109.4 angles. The average P–O distance and bond angle are consistent with those typical values observed in indium phosphates (3, 4, 8–13).

The structural topology of the $(NH_4)In(OH)PO_4$ compound, which is the first ammonium–indium phosphate with a three-dimensional framework, is similar to that found in other indium phosphate compounds $AIn(OH)PO_4$ (A = K, Rb), but the displacement of potassium on ammonium cation leads to an increase of unit cell symmetry from $P2_12_12_1$ to $P4_32_12$, respectively. The structure is characterized by helical chains of *cis*-$InO_4(OH)_2$ octahedra which are connected by OH groups and the chains are interconnected by PO_4 tetrahedra, forming an open framework with infinite tunnels. The ammonium cations are accommodated in the cavities of the framework and control the shape of the channels. The observation of a very low SHG response is consistent with the empirical fact that distorted octahedral $InO_4(OH)_2$ groups are considerably smaller than that in $KTiOPO_4$ and there are no anomalously short In–O bonds in the $(NH_4)In(OH)PO_4$ compound.

ACKNOWLEDGMENTS

This work was partially supported by the Russian Foundation for Basic Research (Grant 00-03-32660). The authors express their gratitude to Dr. S. Yu. Stefanovich (Moscow State University, Russia) for SHG measurements.

REFERENCES

1. A. K. Cheetham, G. Férey, and T. Loiseau, *Chemie. Int. Ed.* **38,** 3268 (1999).
2. M. E. Davis, *Chem. Eur. J.* **3,** 1745 (1997).
3. E. A. Genkina, L. A. Muradyan, B. A. Maksimov, B. V. Merinov, and S. E. Sigarev, *Kristallografiya* **32,** 74 (1987).
4. Q. D. Tran and S. Hamdoune, *Acta Crystallogr. C* **43,** 397 (1987).
5. T. Q. Duc, S. Hamdoune, and Y. Le Page, *Acta Crystallogr. C* **43,** 201 (1987).
6. D. Antenucci, G. Míehe, P. Tarte, W. W. Schmahl, and A.-M. Fransolet, *Eur. J. Mineral.* **5,** 207 (1993).
7. S. S. Dhingra and R. C. Haushalter, *J. Solid State Chem.* **96,** 112 (1994).
8. J. A. Hriljac, C. P. Grey, A. K. Cheetham, P. D. VerNooy, and C. C. Torardi, *J. Solid State Chem.* **123,** 243 (1996).
9. K.-H. Lii, *J. Chem. Soc. Dalton Trans.* 815 (1996).
10. K.-H. Lii, *J. Solid State Inorg. Chem.* **33,** 519 (1996).
11. M. G. Zhizhin, V. A. Morozov, A. P. Bobylev, A. M. Popov, F. M. Spiridonov, L. N. Komissarova, and B. I. Lazoryak, *J. Solid State Chem.* **149,** 99 (2000).
12. J. Winand, A. Rulmont, and P. Tarte, *J. Mater. Sci.* **25,** 4008 (1990).
13. K.-H. Lii and J. Ye, *J. Solid State Chem.* **131,** 131 (1997).
14. X.-J. Tang and A. Lackgar, *Anorg. Allg. Chem.* **622,** 513 (1996).
15. X. Tang, M. J. Gentiletti, A. Lachgar, V. A. Morozov, and B. I. Lazoryak, *Solid State Sci.* **3,** 143 (2001).
16. M. P. Attfield, A. K. Cheetham, and S. Natarajian, *Mater. Res. Bull.* **35,** 1007 (2000).
17. J.-X. Mi, Y.-X. Huang, S.-Y. Mao, X.-D. Huang, Z.-B. Wei, Z.-L. Huang, and J.-T. Zhao, *J. Solid State Chem.* **157,** 213 (2001).
18. M. L. F. Phillips, W. T. A. Harrison, G. D. Stucky, E. M. McCarron, J. C. Calabrese, and T. E. Gier, *Chem. Mater.* **4,** 222 (1992).
19. R. Yu, D. Wang, T. Takei, H. Koizumi, and N. Kumada, *J. Solid State Chem.* **157,** 180 (2001).
20. K. Nakamoto, "Infrared Spectra of Inorganic and Coordination Compounds." Wiley-Interscience, New York, 1986.
21. A.S. Povarennykh, *Am. Min.* **63,** 956 (1978).
22. D. Wang, R. Yu, N. Kumada, and N. Kinomura, *Chem. Mater.* **12,** 956 (2000).
23. P. Tarte, A. M. Fransolet, and F. Pillard, *Bull Min.* **107,** 745 (1984).
24. P.-E. Werner, L. Erriksson, and M. Westdahl, *J. Appl. Crystallogr.* **18,** 367 (1985).
25. V. B. Zlokazov and V. V. Chernyshev, *J. Appl. Crystallogr.* **25,** 447 (1992).
26. H. Torraya, *J. Appl. Crystallogr.* **19,** 440 (1986).
27. W. A. Dollase, *J. Appl. Crystallogr.* **19,** 267 (1986).
28. M. Ahtee, M. Nurmela, P. Suortti, and M. Järvinen, *J. Appl. Crystallogr.* **22,** 261 (1989).
29. M. Järvinen, *J. Appl. Crystallogr.* **26,** 525 (1993).
30. V. V. Chernyshev and H. Schenk, *Z. Kristallogr.* **213,** 1 (1998).
31. T. Loiseau, P. Lacorre, Y. Calage, and G. Férey, *J. Solid State Chem.* **111,** 390 (1994).
32. N. E. Brese and M. O'Keeffe, *Acta Crystallogr. B* **47,** 192 (1991).
33. R. D. Shannon, *Acta Crystallogr. A* **32,** 751 (1976).
34. G. D. Stucky, M. L. F. Phillips, and T. E. Gier, *Chem. Mater.* **1,** 492 (1989).